



ISSN: 0975-833X

Available online at <http://www.journalcra.com>

INTERNATIONAL JOURNAL
OF CURRENT RESEARCH

International Journal of Current Research
Vol. 14, Issue, 03, pp.21120-21126, March, 2022

DOI: <https://doi.org/10.24941/ijcr.43388.03.2022>

RESEARCH ARTICLE

STUDY OF HYBRID GEOTHERMAL COOLING SYSTEM

*A. Nagy Elsayed, M. M. Abo El Nasr and W. Aboelsoud

Mechanical Power Engineering, Ain Shams University, Cairo, Egypt

ARTICLE INFO

Article History:

Received 24th December, 2021

Received in revised form

19th January, 2022

Accepted 24th February, 2022

Published online 30th March, 2022

Keywords:

Geothermal energy, Solar chimney, Shallow geothermal, Hybrid geothermal solar.

*Corresponding author:

A. Nagy Elsayed

ABSTRACT

Using renewable energy for heating and cooling applications covers the increasing demand of energy sources. In the present study, numerical analysis is used to study 9 closed-loop geothermal air pipe system cases during summer and winter with different pipe geometry of diameters of 0.17, 0.35, and 0.65 meters and total pipe lengths of 47, 64 & 87 meters for air conditioning application. The conditioned air is then supplied to a room of Length 3m x Width 3m x Height 3m. The numerical model is combined with a 1 m length solar chimney of 45° inclination angle. Also, an experiment was conducted in Damanhur city, Beheira Governorate, Egypt, providing conditioned air to a room of L 2m x W 2m x H 2m via a 5 m long, 5.3 mm thick geothermal PVC air pipe of 2 inches in diameter. The pipe was buried at 2 m depth and was supported by the solar chimney during winter to provide natural draft force inside the closed-loop system and to support the heating process. On the other hand, the closed loop contains a driving fan to provide circulation during summer. The results of the numerical model prove that the numerical analysis showed the highest level of air conditioning temperature difference close to 5 °C for the case of 0.65 m diameter pipe, and 87 m total length. The validation of the numerical model was carried out using experimental results.

Copyright © 2022. A. Nagy Elsayed et al. This is an open access article distributed under the Creative Commons Attribution License, which permits unrestricted use, distribution, and reproduction in any medium, provided the original work is properly cited.

Citation: A. Nagy Elsayed, M. M. Abo El Nasr and W. Aboelsoud, "Study of Hybrid Geothermal Cooling System", 2022. *International Journal of Current Research*, 14, (03), 21120-21126.

INTRODUCTION

The majority of the building's energy consumption is due to heat, ventilation, and air conditioning (HVAC) systems, which take around 60% of the global energy consumption in the building's sector and 40% for different energy combustion sectors. Evola et al. (2006) study shows that velocity and pressure distribution inside and around the building are determined, as well as the ventilation rate, for three different configurations: cross ventilation, single-sided ventilation with an opening on the windward wall and single-sided ventilation with an opening on the leeward wall. When numerical results are compared with experimental data, showing a good agreement, particularly when using the Renormalization Group (RNG) model, results also show that the north window has the minimum interior temperature, discomfort hours, cooling load, CO₂ emissions, total energy consumption and energy cost, and maximum lighting, relative humidity and heating load and contrarily the southern window. Elghamry et al. (2019) mentioned that window characteristics haven't a great effect on the relative humidity. Increasing the wall area ratio increases the cooling load, interior temperature, energy consumption, and cost and decreases lighting and heating loads. Window shape ratio (2-1) and middle position represent the lowest in

the energy consumption contrarily ratio (1-3) and down position. Kanoglu et al. (1999) point out to the thermal energy in the earth's crust fluid and rock is geothermal energy. The contained energy has three categories, depending on its temperature; low temperature < 90°C, 90°C < moderate temperature < 150°C, and high temperature > 150°C. During the last three decades, geothermal energy gained prominence in electricity production and shallow geothermal applications with direct use. Between 2005 and 2010, there was more than a 20% increase in geothermal power in 24 countries. The generating power from 8933 MW of installed power capacity was 55,709 GWh/year then 67,246 GWh/year was used, from 10,715 MW, for installed power capacity. It continued to increase to 18,500 MW, the study concluded that the need for heating and irrigating a greenhouse is respectively estimated at 0.3 and 0.03 L/s. The rest (the return water) which represents 90% (0.27 L/s) should supply the oases surrounding the area, but this is often difficult to achieve. Fridleifsson et al. (2008) remark about direct use capacity increased by 79% which reached 438,073 TJ/year from 51 GWh/year worldwide, the study concluded that the geothermal utilization sector growing most rapidly is heat pump applications. This development is expected to continue in the future making heat pumps the major direct utilization sector and the CO₂ emission related to

direct applications is negligible and very small in electricity generation compared to using fossil fuel. Currently, new innovative applications generate more efficiencies from low-temperature resources (Dickson, 2003). Geothermal energy is a clean and renewable resource that comes from the earth's crust. Additionally, it acts as an energy potential to generate electric power, which can be used for heat applications and to replace fossil fuels. Many environmental problems are caused by fossil fuels. Decreasing their quantity increases indispensable renewable energy resources. An unparalleled solution like geothermal has characteristics such as adaptability, modularity, safety, and availability, which overbears environmental problems and fossil fuel depletion. These benefits are captivating and both developed and developing countries strive to use geothermal instead of fossil fuel, the study concluded to introduce a methodology to render the comparison of plant efficiencies on common input and environmental conditions, even though the plants being compared operate with somewhat different fluid inlet and ambient temperatures (DiPippo, 2004).

Climate change remains one of the biggest concerns in many countries. A Geothermal composition may help achieve the highest efficiency (Dincer, 2011). Using applications less than 400 m in depth, "shallow geothermal" is the most common system worldwide because it does not require complicated technologies or high temperatures in deep layers of the earth that require extraordinary geological regulations. Moreover, conventional air conditioners harm the environment, a feature shallow geothermal energy does not suffer from. As such, it is convenient for domestic air conditioning applications, Man et al. (2011) study indicated that it is feasible to use a nocturnal cooling radiator to serve as a supplemental heat rejecter of the novel hybrid ground-coupled heat pump system for cooling load dominated buildings even those located in humid subtropical climate areas.

Geothermal itself is a free and renewable source of energy all year, whatever global energy market status. This makes relying on thermal energy the logical choice as a power generation source, cooling, heating, agricultural applications, energy storage, water desalination, fish farming, health and balneological systems. When geothermal energy is compared with other renewable energy sources, it involves the lowest capital costs for decreased fossil fuel use. Geothermal energy is available at all times and during all circumstances for the consumer. Renewable geothermal energy establishes the foundation for a supply of resources, making it favorable to use as renewable energy and as the primary provenance of required power in a project or application, the study refers to the experimental results obtained are satisfying to develop this technique in the near future for supply population in these regions where the geothermal water, clean and free energy, exists on abundance (Ozgener, 2007).

Geothermal energy has many applications such as greenhouses air conditioning and heating crops roots in open areas. Even after growth, it can be used for drying vegetables, fruits, and wood. Geothermal energy is useful in adjusting the temperature in fisheries and drying fish. Furthermore, geothermal resources are available in agricultural zones, which is ideal instead of other kinds of energy sources like fossil fuels. By using geothermal energy in greenhouses, out-of-season products can be produced at any time as geothermal energy provides stable temperature throughout the year (Albright, 1991).

Mahmoud et al. (2017) performed a numerical study on the enhancement of earth-to-air heat exchanger heat transfer using porous media, the study conclude that for laminar flow an enhancement in the bulk temperature difference across the EAHE of up to 25 % can be achieved using only 10 mm thickness of carbon foam V-shaped insert. Results also show that changing the apex angle of the V-shaped insert can significantly reduce the pressure drop across the porous insert. A volume saving of up to 40 % can be obtained in the EAHE by using the V-shaped configurations. Many other studies examined the performance of using a solar chimney for natural ventilation. For 25 years, many countries used geothermal energy to provide conditioned air for greenhouse applications and provide a stable source of energy throughout the year, noting that geothermal energy is not affected by outside weather temperature. In this study, an analysis will be performed on the thermal performance of a hybrid geothermal-solar energy system to control the air temperature in a closed environment and conduct an experiment to obtain relationships between the controlling parameters and recommend the dimensionless form relationship that achieves the best thermal performance.

Numerical analysis: The first step is to choose a depth for the application. There was an attempt to establish a depth of 12 meters in the analysis. However, different research and experimental studies in Turkey (Onder Ozgener, 2010) and Egypt in which the study showed that using an ETAHE system for the heating of a greenhouse was more efficient and low cost compared to using it for cooling in all cases of pipe diameters (Shaban Gaber Ali Gouda, 2010) used different depths that start from 1 to 4 meters. Therefore, it is recommended to implement a 4-meter depth in the current study, where the temperature is constant at 20 °C. This work is conducted on 3d transient computational fluid dynamics simulations for geothermal room heating with three different pipe length designs. The boundary condition was set as shown in Table 1. Table 2. Shows the initial data of the underground pipe length for the first iteration was 31 m, 51 m for the second, and 71 m for the third. The transient response of the room's volume average temperature was investigated to examine the effect of pipe length on the volume average temperature. The computational domain constituted of a 3m x 3m x 3m room, a chimney, and connection pipe to the underground.

Basic data of all cases including chimney:

Room dimensions in meters = L X W x H = 3 X 3 X 3, surface area = $6 \times 3^2 = 54 \text{ m}^2$

Chimney is 1 m in length

Underground connection pipes = 3.575 m x 2 pipes = 7.15 m
Top (above ground surface) connection pipes = 3.884 + 0.56 + 1.25 + 0.56 + 0.075 + 0.56 + 0.37 + 0.2 = 7.459 m as shown in Fig. 1.

Underground connection pipes = 3.575 m x 2 pipes = 7.15 m
Top (above ground surface) connection pipes = 3.884 + 0.56 + 1.25 + 0.56 + 0.075 + 0.56 + 0.37 + 0.2 = 7.459 m as shown in Fig. 1. The study examines the effect of pipe diameters and underground pipe length on conditioning room temperature and using the solar chimney to drift air through it. This results in the natural circulation of air, heating the air, and establishing

the geothermal effect on the underground pipe. The time scale was massive during the run. This was implemented on the system based on numerical analysis, which was close to 2000 seconds in each case.

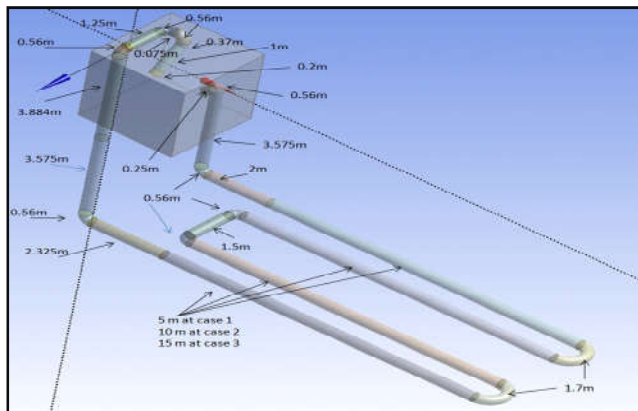


Fig. 1. System length dimensions

It took more than 15 days for each case to obtain results because of the length and diameters of the pipes, including room dimensions as well. The air temperature inside the room was measured as an average.

Discretization: Different meshes were generated in this numerical analysis. The model uses 157245 hexahedra elements with max skewness of 3.28115, an aspect ratio of 128.081, and a minimum volume of $2.7286e-09 \text{ m}^3$, the convergence criterion was achieved when the relative error of the temperature change is less than 0.001. Adding a fresh air inlet to each case separately results in a system without a chimney case as shown in Fig. 2.

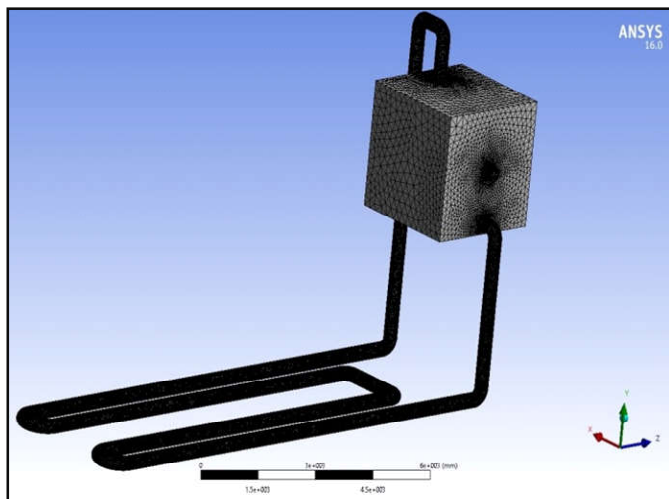


Fig. 2. Fresh air inlet in summer system mesh design

During summer, it uses electric AC 55 watts and a 20 cm diameter blower, as shown in Fig. 3. instead of the chimney to avoid unwanted temperature increase.

The design is a closed-loop, including the solar chimney and electric air blower. There is a bypass for the solar chimney to prevent air from passing through it when it is not required during summer. This can be controlled by valves. In addition, there is an inlet gate that allows fresh air to pass in as a result of pressure difference from the system vacuum effect.

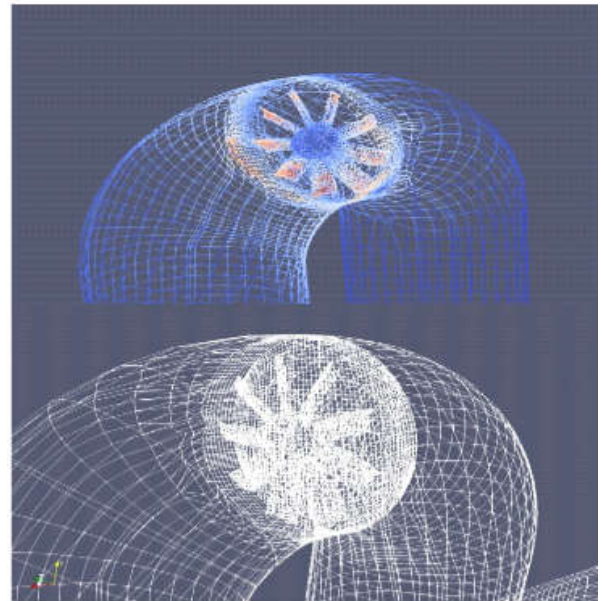


Fig. 3. System air blower

Experimental work: An experiment was conducted for validation of numerical results, in Damanhur, Egypt, with longitude and latitude of $31^{\circ}01'50.7'' \text{ N}$ and $30^{\circ}26'49.5'' \text{ E}$ respectively as shown in Fig. 4.



Fig. 4. (a) Room and solar chimney during construction step & (b) Closed-loop experimental system running and in use

The solar chimney consists of 0.3 m width air gap thickness, front glass of 5 mm in thickness supported by 10 mm wood hood was placed with an angle of 45° , 1.6 m long 0.7 m. In addition, its base was painted black to increase the emission from the surface. the sides of the chimney are insulated by a 0.6 m Styrofoam material 0.03 W/ m.K , characterized by low thermal conductivity, and the bottom of the chimney was insulated by glass wool of 25 mm thickness, density 16 kg/m^3 & 0.04 W/ m.K , with low thermal conductivity. It is attached to the cubic room with the dimensions of $2 \text{ W} \times 2 \text{ L} \times 2 \text{ H}$ meters manufactured by 10 mm thickness wood and covered by Styrofoam 12 cm thickness to act as insulation. A 5-meter-long PVC tube 2 inches in diameter 5.3 mm in thickness was buried at 2 m depth as shown in Fig. 5. It is connected 0.2 m above ground to the room. The other side of the pipe is connected in 2 ways; the first is attached to the chimney and the second is a bypass for the chimney, where the pipe connects to the room ceiling Two valves are used to control the chimney connection pipeline and its bypass pipeline. All earth outside pipeline connections is insulated by glass wool. The room has a door of 172 cm in height and 59 cm in width. It is usually closed and is only used just used to shut off the system before checking room internal sensors, closing/opening chimney inlet, or closing/opening bypass line inlet. A window of 0.8 m in height x 0.8 m in width was in the same wall

containing the air inlet pipe. the window is 0.2 m from the ceiling and is located in the middle of the wall. It is usually closed, which allows the system to act as a closed loop. However, some experiments had an open window for ventilation and adjusting the air quality level inside the room while running the close loop system. “Ebmpapst” model number G2S097AA03.03 55 watts 0.3 amperes 220 volts 2480 rpm air blower is attached to the connection point between chimney outlet and its bypass line. The air temperature inside the room was measured at the middle of the room.



Fig. 5. Installing geothermal pipe

Validation: In this study, the process of conditioning air using a hybrid geothermal-solar system will be investigated. The thermal performance of a hybrid geothermal-solar energy system to control the air temperature in a closed environment will be analyzed. This analysis includes changing: the pipe length, diameter, depth, air flow rate, and height and angle of the solar chimney.

The experimental and numerical work aim to obtain relationships between the parameters under study. Results will then be presented in a recommended dimensionless form to obtain the best thermal performance. Finally, validation of numerical results with experimental data. Different pipe geometries were used in the numerical and experimental studies as shown in Tables (3, and 4), which show the proposed pipe diameters and lengths under study. A range of different diameters and lengths varying from 0.17 m to 0.65 m, and from 47 m to 87 m respectively were used to carry out the study. To validate the numerical model, a dimensionless temperature Θ was defined, that is (Temperature of outside weather - Minimum temperature of the room) / (Maximum temperature of the room - Minimum temperature of the room). The dimensionless temperature Θ was plotted versus time as shown in Figure (6)

RESULTS AND DISCUSSION

By combining the effects of the solar chimney and geothermal application, the total system performance is improved, as the chimney improves air circulation, the time required to heat the air, finding relations between all system parameters, including air flow rate and time required for air conditioning.

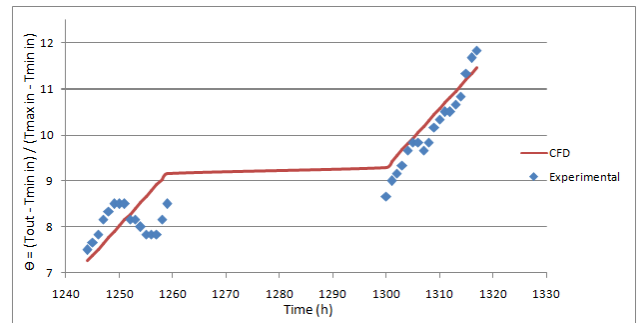


Fig. 6. Validation pipe size 31 m length & 17 cm diameter.

This gives more control to the system and allows us to set parameter boundaries during design and the system operation stage to obtain the target temperature in the least amount of time.

Case 1: Underground effective pipes = (5 m x 4 pipes) + 11.465 m = 31.465 m

Total pipes length including chimney = 31.465 + 7.15 + 7.459 + 1 = 47.074 m

Study 1.1 : Pipe / Chimney 0.17 m diameter

Study 1.2 : Pipe / Chimney 0.35 m diameter

Study 1.3 : Pipe / Chimney 0.65 m diameter

Case 2 Underground effective pipes = (10 m x 4 pipes) + 11.465 m = 51.465 m

Total pipes length including chimney = 51.465 + 7.15 + 7.459 + 1 = 67.074 m

Study 2.1 : Pipe / Chimney 0.17 m diameter

Study 2.2 : Pipe / Chimney 0.35 m diameter

Study 2.3 : Pipe / Chimney 0.65 m diameter

Case 3 Underground effective pipes = (15 m x 4 pipes) + 11.465 m = 71.465 m

Total pipes length including chimney = 71.465 + 7.15 + 7.459 + 1 = 87.074 m

Study 3.1 : Pipe / Chimney 0.17 m diameter

Study 3.2 Pipe / Chimney 0.35 m diameter Study 3.3 : Pipe / Chimney 0.65 m diameter

Figure (7) show that using a 17 cm diameter pipe with a 31-meter length, the room temperature reaches a steady state after 14 minutes, and the maximum temperature is achieved after 33 minutes, the room temperature trend affected by both outside temperature and the underground (geothermal) temperature. By increasing the pipe length to 51- meters with the same pipe diameter, the temperature increases by 1 celsius in 11 minutes, and then the steady-state temperature is reached after 3 minutes, and the maximum temperature is achieved at 28 minutes. Figure (8) shows that the maximum temperature difference of 6.5 occurs for the 17 cm diameter pipe of 31-meter length, the minimum temperature difference is 4.5 for the 17 cm diameter pipe of 51-meter length. Figure (9) shows that using a 31-meter length pipe that is 35 cm in diameter, the time required for the flow rate to reach 0.048 kg/sec is 31 seconds. Then, it decreases to 0.04 in 336 seconds and becomes steady.

Table 1. Boundary and initial conditions (BC & IC)

	Fluid flow	Thermal
Room (IC)	Wall (no-slip)	Isothermal t=285 k (12 C)
Connection pipe (atmospheric) (BC)	Wall (no-slip)	Adiabatic (Q=0)
Connection pipe (underground) (BC)	Wall (no-slip)	Adiabatic (Q=0)
Underground pipe (soil surface) (BC)	Wall (no-slip)	Isothermal t=293 k (20 C)
Chimney (BC)	Wall (no-slip)	Solar Heat flux (400 watt/m2)

Table 2. First calculations and initial data

Rayleigh number = $Gr * Pr$ (If Rayleigh number $< 10^9$ the flow is Laminar) (If Rayleigh number $> 10^9$ the flow is Turbulent)	Ra	4.13E+10
Grashof number = $(g \beta (\Delta T) L^3) / \nu^2$	Gr	5.90E+10
Prandtl number	Pr (Air)	0.7
Acceleration of gravity	g (m/s ²)	9.81
Thermal expansion coefficient (1 / T (Kelvin) "Average Range")	β	0.0033151
(Input) Room Temperature	T1 Kelvin	310.15
(Input) Pipe Temperature	T2 Kelvin	293.15
	Avg ΔT	301.65
(Input) Characteristic length	L (Room) Meter	3
(Input) Kinematic viscosity	ν (x10 ⁻⁵ m ² /s)	1.59
The smallest cell size	Δx (mm)	1
Velocity	u (m/s)	0.001
Time step $< \Delta x/u$	Δt (mm / (m/s))	950
Courant-Friedrichs-Levy number = $u * \Delta t / \Delta x$	CFL	1

Table 3. Parameters of numerical analysis

CFD RESULTS	DIAMETER D, LENGTH L								
	D 0.17 , L 47.047	D 0.17 , L 64.074	D 0.17 , L 87.074	D 0.35 , L 47.047	D 0.35 , L 64.074	D 0.35 , L 87.074	D 0.65 , L 47.047	D 0.65 , L 64.074	D 0.65 , L 87.074
Reynolds Number Winter (Rn)	4673	3865	4140	5975	5789	5690	10058	11042	11036
Reynolds Number Summer (Rn)				7660	7097	6314	11870	13074	8552
Relative Roughness	0.000882	0.000882	0.000882	0.000429	0.000429	0.000429	0.000231	0.000231	0.000231
Absolute Roughness ϵ (0.15 mm) / Velocity	0.000343	0.000415	0.000387	0.000553	0.000570	0.000580	0.000610	0.000555	0.000556
Nusselt number (Nu)	22.44	22.44	22.44	42	42	42	75.4	75.4	75.4
L/D	277	395	512	135	192	249	72	103	134

Table 4. Experimental PVC Pipe diameter and length size study

EXPERIMENTAL SIZE STUDY USING PVC	Pipe Diameter (INCH)										L/D
	0.25	0.5	0.75	1	1.25	1.5	1.75	2	2.25		
	Pipe Diameter (METER)										
	0.0064	0.0127	0.01905	0.0254	0.03175	0.0381	0.04445	0.0508	0.05715		
Total Pipe Length (METER)	1	157	79	52	39	31	26	22	20	17	
	2	315	157	105	79	63	52	45	39	35	
	3	472	236	157	118	94	79	67	59	52	
	4	630	315	210	157	126	105	90	79	70	
	5	787	394	262	197	157	131	112	98	87	
	6	945	472	315	236	189	157	135	118	105	
	7	1102	551	367	276	220	184	157	138	122	
	8	1260	630	420	315	252	210	180	157	140	
	9	1417	709	472	354	283	236	202	177	157	
	10	1575	787	525	394	315	262	225	197	175	
	11	1732	866	577	433	346	289	247	217	192	
	12	1890	945	630	472	378	315	270	236	210	
	13	2047	1024	682	512	409.4	341	292	256	227	
	14	2205	1102	735	551	441	367	315	276	245	

Using a 51-meter length pipe and 35 cm in diameter, the time required for the flow rate to reach 0.044 kg/sec is 31 seconds, which decreases to 0.038 in 446 seconds and becomes steady. Furthermore, using a 71-meter length pipe and 35 cm in diameter, the time required for the flow rate to reach 0.039 kg/sec is 31 seconds. It then decreases to 0.033 in 590 seconds and becomes steady. If we use a 31-meter length pipe and 65 cm in diameter, the time required for the flow rate to reach 0.13 kg/sec is 21 seconds, which decreases to 0.11 in 462 seconds and becomes steady.

To add, using a 51-meter length pipe and 65 cm in diameter, the time required for the flow rate to reach 0.15 kg/sec is 25 seconds which decreases to 0.13 in 407 seconds and becomes steady later on. Finally, using a 71-meter length pipe and 65 cm in diameter, the time required for the flow rate to reach 0.1 kg/sec is 22 seconds, which decreases to 0.085 in 365 seconds and becomes steady. Fig. 10. shows the relationship between the mass flow rate and temperature difference, where the maximum flow rate of 0.048 kg /s is achieved at a temperature difference of 4.5, then the flow rate decrease gradually with the

temperature difference increase, and then the steady-state flow is reached at 5 temperature difference.

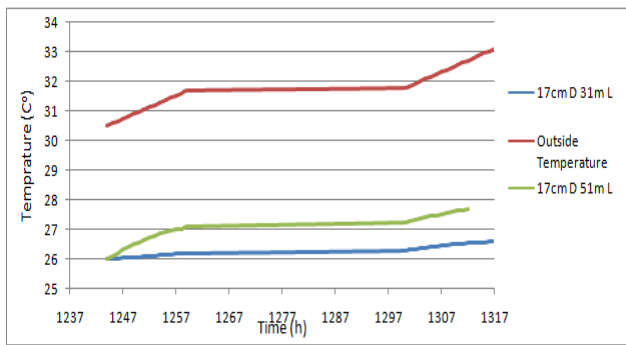


Fig. 7. Temperature vs time in summer operating condition

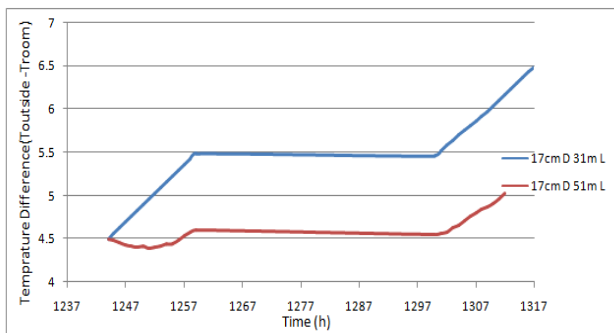


Fig. 8. Temperature difference vs time in summer operating condition

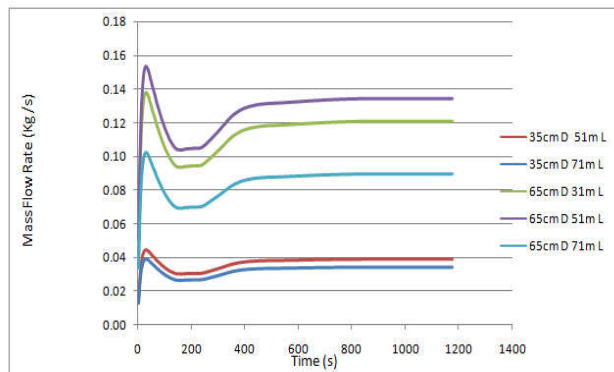


Fig. 9. Mass flow rate vs time in summer operating condition

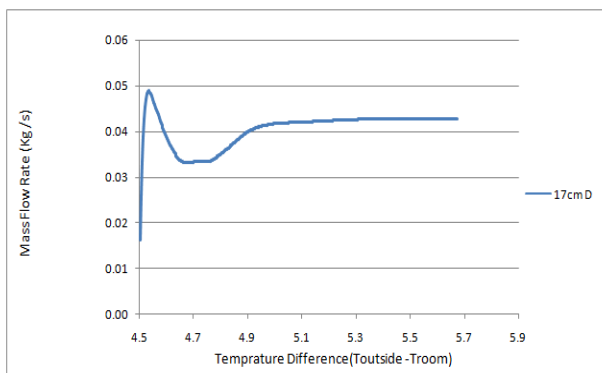


Fig. 10. Mass flow rate vs temperature difference in summer operating condition

CONCLUSION

The chimney helps in improving air circulation, the time required to heat the air, finding relations between all system parameters, including air flow rate and time required for air conditioning and gives more control over the system. To add, It allows us to set parameter boundaries during the design and system operation stage to obtain the target temperature in the least amount of time possible. To conclude, our findings highlight that the results obtained from some pipe diameters that are close to each other, like one with a diameter of 65 cm and lengths of 31 m & 51 m, means that selecting a pipe with 31 m is cost-efficient and provides the same target results as the one with a diameter of 35 cm, with both pipe lengths of 51 m & 71 m. During winter conditions the maximum temperature difference that can be achieved with the proposed design is 4.8 while in summer conditions it is 5.7.

REFERENCES

- Evola, G., Popov, V., 2006. Computational analysis of wind-driven natural ventilation in buildings. *Energy Build.* 38, 491–501. <https://doi.org/10.1016/j.enbuild.2005.08.008>.
- Elghamry, R., Hassan, H., 2019. Impact of window parameters on the building envelope on the thermal comfort, energy consumption, cost, and environment. *Int. J. Vent.* 1–27. <https://doi.org/10.1080/14733315.2019.1665784>.
- Kanoglu M, Cengel YA. Economic evaluation of geothermal power generation, heating, and cooling. *Energy* 1999;24(6):501–9.
- I.B. Fridleifsson, R. Bertani, E. Huenges, J.W. Lund, A. Ragnarsson, L. Rybach, The possible role and contribution of geothermal energy to the mitigation of climate change Luebeck, Germany, in: O. Hohmeyer, T. Trittin (Eds.), *IPCC Scoping Meeting on Renewable Energy Sources, Proceedings (2008)*, pp. 59e80 Available online at: http://iga.igg.cnr.it/documenti/IGA/Fridleifsson_et_al_IPCC_Geothermal_Paper_2008.pdf.
- Dickson M, Fanelli M. Geothermal background. In: Dickson MH, Fanelli M, editors. *Geothermal energy: utilization and technology*. UNESCO renewable energy series. Earthscan Publications Ltd.; 2003.
- DiPippo, R. Second law assessment of binary plants for power generation from low-temperature geothermal fluids, *Geothermics* 33 (2004) 565-586.
- Dincer I, Rosen M. *Thermal energy storage: systems and applications*. 2nd ed. London: Wiley; 2011.
- Man Y, Yang H, Spitler J, Fang Z. Feasibility study on novel hybrid ground-coupled heat pump system with nocturnal cooling radiator for cooling load dominated buildings. *Appl Energy* 2011;88:4160–71.
- Ozgener L, Hepbasli A, Dincer I. Parametric study of the effect of dead state on energy and exergy efficiencies of geothermal district heating systems. *Heat Transfer Eng* 2007;28(4):357–64.
- Albright LD. 1991. Production solar greenhouses. In: Parker BF, editor. *Solar energy in agriculture*. New York: Elsevier, 1991.
- Mahmoud, Y. E.W. Aboelsoud, M. M. Kamal, and A. M. El Baz, "Numerical study of heat transfer enhancement of earth-to-air heat exchanger using porous media," *Int. Symp. Adv. Comput. Heat Transf.*, pp. 1849–1860, 2017, <https://doi.org/10.1615/ichmt.2017.cht-7.1970>

Onder Ozgener a, Leyla Ozgener . Exergoeconomic analysis of an underground air tunnel system for greenhouse cooling system. Elsevier, International Journal of Refrigeration 33 (2010) 995-1005

Shaban Gaber Ali Gouda " using of geothermal energy in heating and cooling of agricultural structures" M.Sc. Thesis, Agricultural engineering department , Faculty of Agriculture, Benha Univ., Egypt. 2010
